

Short communication

Synthesis and sintering of Y_2O_3 -doped ZrO_2 powders using two Pechini-type gel routesEdson Cezar Grzebielucka, Adriana Scoton Antonio Chinelatto,
Sergio Mazurek Tebcherani, Adilson Luiz Chinelatto*

Department of Materials Engineering, State University of Ponta Grossa, Av. Carlos Cavalcanti 4748, Ponta Grossa, Paraná 84030-900, Brazil

Received 17 November 2009; received in revised form 10 January 2010; accepted 22 February 2010

Available online 25 March 2010

Abstract

Yttria-tetragonal zirconia polycrystal ($\text{ZrO}_2 + 4.5 \text{ mol\% Y}_2\text{O}_3$) nanocrystalline powder was synthesized by two Pechini-type gel routes, the *in situ* polymerized complex (IPC) method and the PEG/AF method. FTIR spectra confirmed coordination of metal ions with the polymer by different routes, depending on the method used. The crystallite size of the powder increased from 5 nm to 8 nm when the temperature was increased from 450 °C to 600 °C and calcination times increased from 2 h to 24 h. The morphology of the powders differed only when the organic impurities were not completely eliminated. After calcination, the morphology of the powders produced by the two methods showed porous agglomerates composed of smaller particles. All the resulting microstructures were very similar, regardless of the method employed to obtain the powder or the calcination times and temperatures.

© 2010 Elsevier Ltd and Techna Group S.r.l. All rights reserved.

Keywords: ZrO_2 ; Calcination behaviors; Tetragonal zirconia polycrystal; Sintering; Chemical powder preparation

1. Introduction

Zirconia has attracted the attention of many scientists due to its excellent mechanical and electrical properties [1–4]. Among its possible applications, the one that has gained the greatest attention is its use in solid oxide fuel cells (SOFC) [3,5,6]. The dopant normally used in SOFC applications is Y_2O_3 , due to the ionic conductivity generated by the replacement of Zr^{4+} by Y [6,7]. ZrO_2 compositions containing more than 8 mol% Y_2O_3 stabilize the cubic phase at room temperature, while compositions containing 2–3% stabilize the tetragonal phase, and compositions between these values generate a mixture of tetragonal and cubic phases [8]. In yttria-tetragonal zirconia polycrystal (Y-TZP) and yttria-partially stabilized zirconia (Y-PSZ), the presence of the tetragonal phase is responsible for increasing the toughness of ceramics [4].

With the advent of nanotechnology, several techniques have been employed to obtain ceramic powders with nanometric dimensions from chemical processes. Chemical synthesis allows the manipulation of matter at the molecular level, enabling good chemical homogeneity, and allows for the control of particle size and shape [9].

The Pechini method [10] is a chemical route to produce powder-based polymeric precursors (*in situ* polymerized complex method—IPC). By this method, metal ions are immobilized in a polymer resin composed of citric acid and ethylene glycol. The metal ions are dispersed uniformly throughout the polymer chain. Another method based on the Pechini route is the PEG/AF method [11,12], which involves the use of polyethylene glycol and formic acid to form polymeric resin in which the metal ions are dispersed.

To obtain ceramic powders by the IPC and PEG methods require the removal of organic impurities through calcination [11–13]. The characteristics of the powder formed by these processes are influenced by the way in which the ions are bound to the polymer and by the calcination time and temperature.

This work involved a study of the effects of calcination time and temperature on the production of Y-TZP powder, and the effect of sintering on the grain morphology of sintered bodies.

* Corresponding author. Tel.: +55 42 3220 3079.

E-mail addresses: edson_cezar@yahoo.com.br (E.C. Grzebielucka), adriana@uepg.br (A.S.A. Chinelatto), sergiomt@uepg.br (S.M. Tebcherani), adilson@uepg.br (A.L. Chinelatto).

2. Experimental procedure

Nanosized powders were produced by two chemical synthesis routes based on the Pechini method, the Pechini (IPC) and the PEG/AF [11–13]. Powders with a $\text{ZrO}_2 + 4.5$ mol% Y_2O_3 composition were prepared by these two methods.

Pechini method (IPC)—Zirconium oxychloride octahydrate ($\text{ZrOCl}_2 \cdot 8\text{H}_2\text{O}$) (VETEC) and yttrium nitrate hexahydrate ($\text{Y}(\text{NO}_3)_3 \cdot 6\text{H}_2\text{O}$) (RIEDEL) were dissolved in ethylene glycol (REAGEN) and anhydrous citric acid (SYNTH) was added. The mixture was stirred for about 30 min while heating to 80°C in order to promote polyesterification.

Method PEG/AF—Zirconium oxychloride octahydrate ($\text{ZrOCl}_2 \cdot 8\text{H}_2\text{O}$) and yttrium nitrate hexahydrate ($\text{Y}(\text{NO}_3)_3 \cdot 6\text{H}_2\text{O}$) were dissolved in formic acid (REAGEN), followed by the addition of polyethylene glycol (MW ≈ 1500 g/mol) (CRQ). After complete dissolution of the polymer, the mixture was kept under agitation for about 30 min.

After synthesis, the two resins were held at 105°C for 24 h to remove water produced during the synthesis. The resins were then analyzed by infrared spectroscopy. Prior to calcination, the IPC resin was heated to 300°C for 90 min. The resins were calcined at 450°C , 500°C , 550°C and 600°C for 2 h, 10 h and 24 h.

After calcination, the powders were ground in an agate mortar. Samples of the two powders were then characterized by scanning electron microscopy (SEM) and X-ray diffraction (XRD) to analyze their phase formation and measure their crystallite size by the Scherrer method [14].

For the determination of the sample and standard, we used the (1 1 1) peak, which is the most intense peak of yttria-doped zirconia. The X-ray diffraction spectra were recorded at a rate of $0.06^\circ \text{ min}^{-1}$ [15].

The milled powders were compacted into cylindrical test specimens under 590 MPa. The powders obtained by the two routes were sintered at 1600°C for 2 h. The sintered bodies were characterized by Fourier transform infrared spectroscopy (FTIR), apparent density, X-ray diffraction (XRD) and scanning electron microscopy (SEM).

3. Results and discussion

The FTIR spectra of resins produced by the Pechini (IPC) and PEG/AF methods are shown in Fig. 1. These spectra indicate that the metal ions coordinated with the polymer in different ways, depending on the method used.

The spectrum of the IPC resin shows a band at 1741 cm^{-1} , which can be attributed to $\text{C}=\text{O}$ [16] axial deformation resulting from the ester formed by condensation reaction with ethylene glycol and subsequent polymerization. Another band is visible in the region between 1641 and 1592 cm^{-1} , which, according Silverstein [17], is characteristic of the group of carboxylate ions, or a metal ion that reacts with the oxygen adjacent to the citric acid anhydrous carboxyl used as reagent. Thus, this full wavelength illustrates that coordination of metal ions occurred during the synthesis of the polymer. Vibration of $\text{C}-\text{O}$ axial deformation of the esters was detected in the band

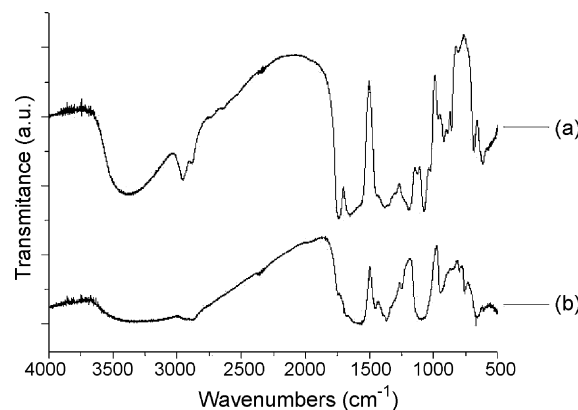


Fig. 1. FTIR spectra of resins (a) and IPC (b) PEG/AF.

from 1189 cm^{-1} , as well as two asymmetrically coupled vibrations: $\text{C}-\text{C}(=\text{O})-\text{O}$, between the bands at 1300 cm^{-1} and 1000 cm^{-1} , which characterize this type of vibration. A very broad band with a peak at 3383 cm^{-1} was also visible, corresponding to symmetric and asymmetric stretching of the $\text{O}-\text{H}$ bonds of water molecules, as well as a peak at 2957 cm^{-1} corresponding to the axial deformation of the reference $\text{C}-\text{H}$.

The difference between the two spectra is demonstrated by the presence or absence of the peak of formation of the ester functional group, which is not formed in chemical reactions by the PEG/AF method. Similarly, the PEG/AF spectrum shows a broad absorption band with a peak at 1587 cm^{-1} , which characterizes the absorption of carboxylate ions resulting from the reaction of formic acid molecules with zirconia and yttria salts. This spectrum also shows a band associated with the asymmetric axial deformation observed at 1370 cm^{-1} , formed by the vibrations between coupled $\text{C}=\text{O}$ and $\text{C}-\text{O}$ [18]. The PEG/AF spectrum of the resin also shows a low intensity peak at 3246 cm^{-1} corresponding to symmetric and asymmetric stretching of $\text{O}-\text{H}$ bonds of water molecules [19] and axial deformation of the $\text{C}-\text{H}$ at 2919 cm^{-1} .

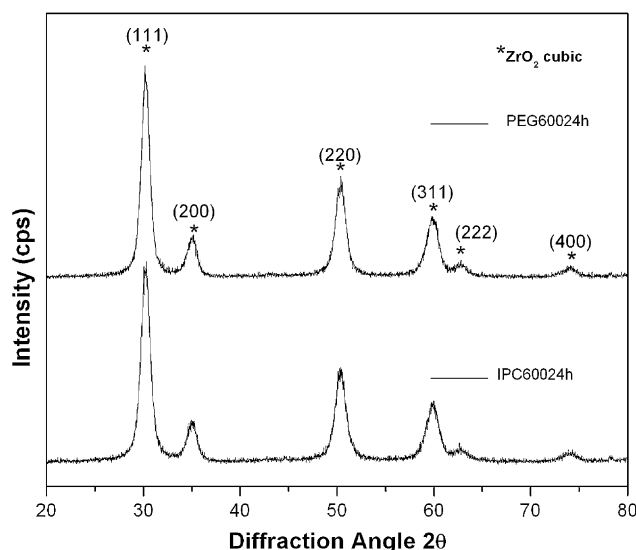


Fig. 2. X-ray diffraction powder resins obtained by calcination at 600°C for 24 h.

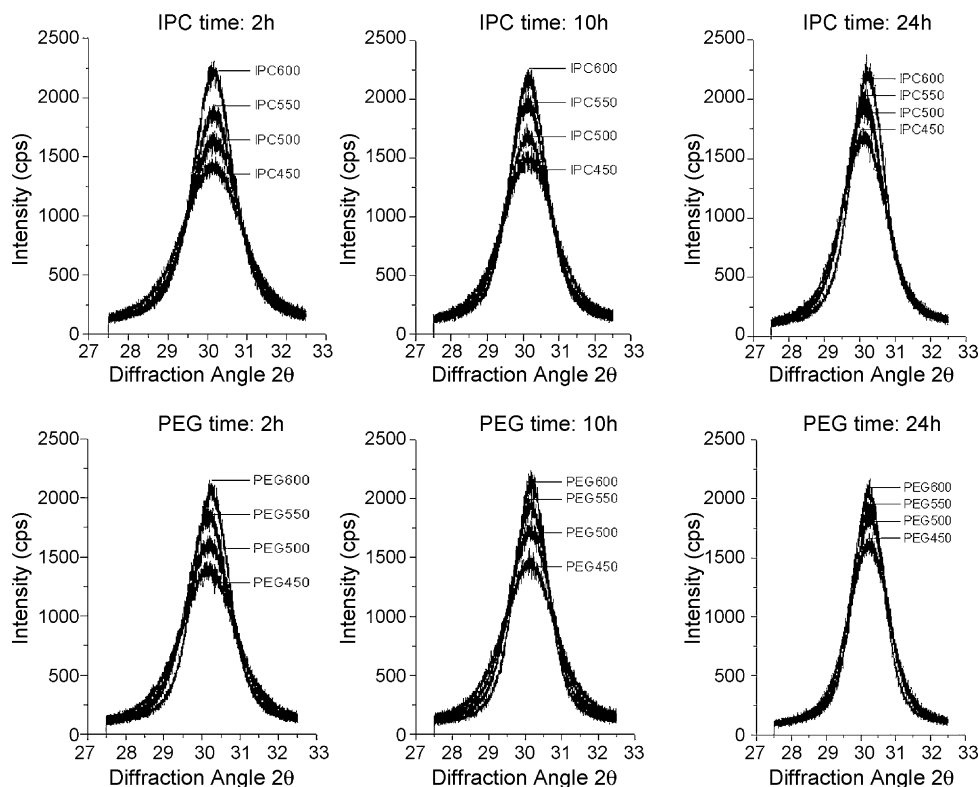


Fig. 3. X-ray diffraction of powders, plane (1 1 1), comparing the evolution of crystallinity with increasing temperature and time by the IPC and PEG/AF methods.

The X-ray diffraction of the powders obtained by the two synthesis methods indicates only the presence of cubic phase of zirconia at all the calcination temperatures applied here. Fig. 2 shows the X-ray diffraction pattern of powders obtained by the PEG/AF and IPC methods and calcined at 600 °C for 24 h.

Fig. 3 shows the most intense (1 1 1) peak in the X-ray diffraction patterns recorded at all the calcination temperatures and times. This figure indicates that variations occurred in the intensity and width at half height, depending on the calcination temperatures and times. These variations were attributed to differences in the crystallite sizes produced by each method. Note that the most significant changes occurred when the temperature was increased from 450 °C to 600 °C and calcination time was 2 h, while the smallest variations occurred in 24 h of calcination.

The crystallite sizes shown in Fig. 4 were determined from an XRD analysis, while the heights of the peaks shown in Fig. 3 were determined using Scherrer's equation. The crystallite size of zirconia was found to increase with rising calcination temperature, regardless of the method used. On average, the PEG/AF showed larger crystallite sizes than the IPC at the same calcination temperatures and times. The powders' crystallite size grew from 5 nm to 8 nm when the temperature was increased from 450 °C to 600 °C and calcination times increased from 2 h to 24 h.

Fig. 5 shows micrographs of the powders produced by the IPC and PEG methods, calcined at 450 °C and 600 °C for 2 h and 24 h.

The powders produced by the IPC method showed porous agglomerates or clusters composed of small particles. This morphology remained unchanged at all the calcination times and temperatures applied. After 2 h of calcination, the clusters displayed a rough surface, but the definite shape of the particles in these clusters remained indeterminate. However, after 24 h of calcination, the clusters clearly showed smaller particles tending toward a spherical shape. These results indicate that even at a calcination temperature of 600 °C, 2 h of calcination was still insufficient to remove all the organic impurities, generating these clusters with rough surfaces.

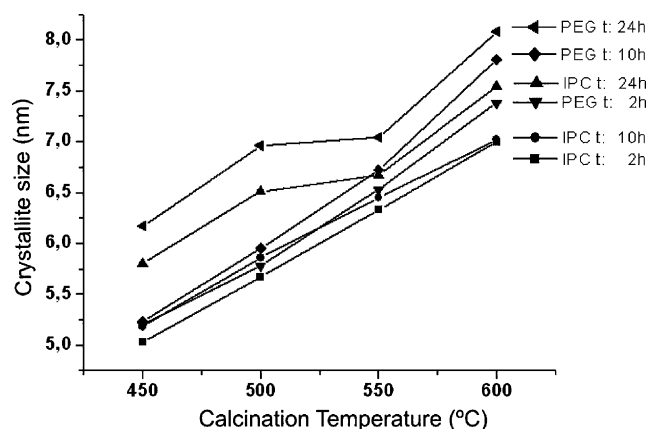


Fig. 4. Crystallite size according to the synthesis route, calcination time and temperature, calculated by the Scherrer method.

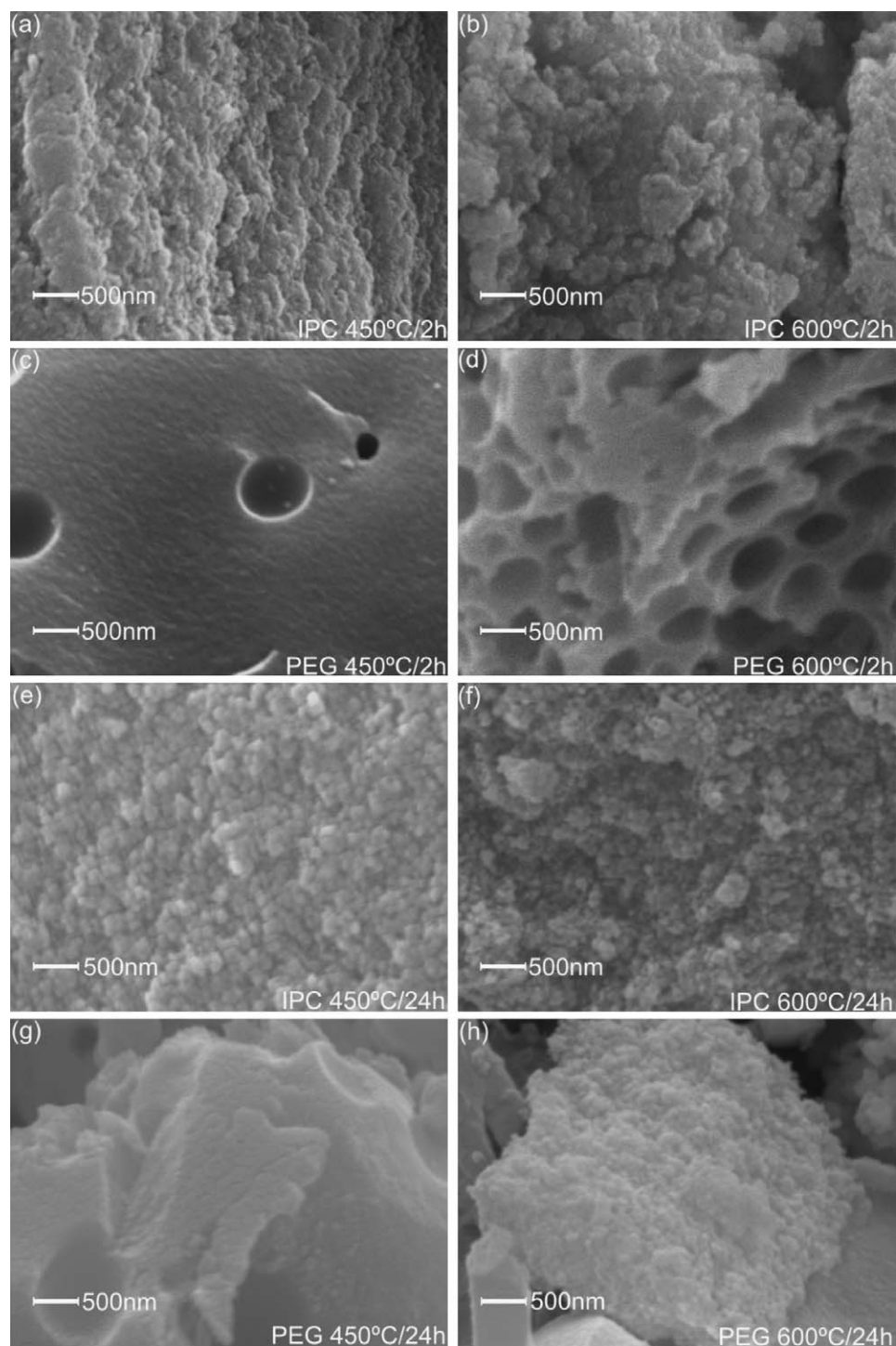


Fig. 5. Comparison of SEM micrographs of the powders produced by the IPC and PEG methods, showing the extremes of calcination temperature applied for 2 h and 24 h: (a) IPC 450 °C/2 h, (b) IPC 600 °C/2 h, (c) PEG 450 °C/2 h, (d) PEG 600 °C/2 h, (e) IPC 450 °C/24 h, (f) IPC 600 °C/24 h, (g) PEG 450 °C/24 h, and (h) PEG 600 °C/24 h.

The PEG powders calcined for 2 h showed a structure of particles with smooth surfaces and spherical sponge-like pores. This morphology resulted from the partial release of organic impurities. After calcination at 450 °C for 24 h the morphology still looked spongy, but with a larger quantity of spherical pores. Calcination at 600 °C for 2 h resulted in a morphology of

particles with rougher surfaces and numerous spherical pores. PEG powders calcined at 600 °C for 24 h displayed a morphology similar to that of the IPC powder.

The powders were pressed into pellets under a pressure of 590 MPa and sintered at 1600 °C for 2 h. It was found that the presence of clusters prevented the densification of the samples.

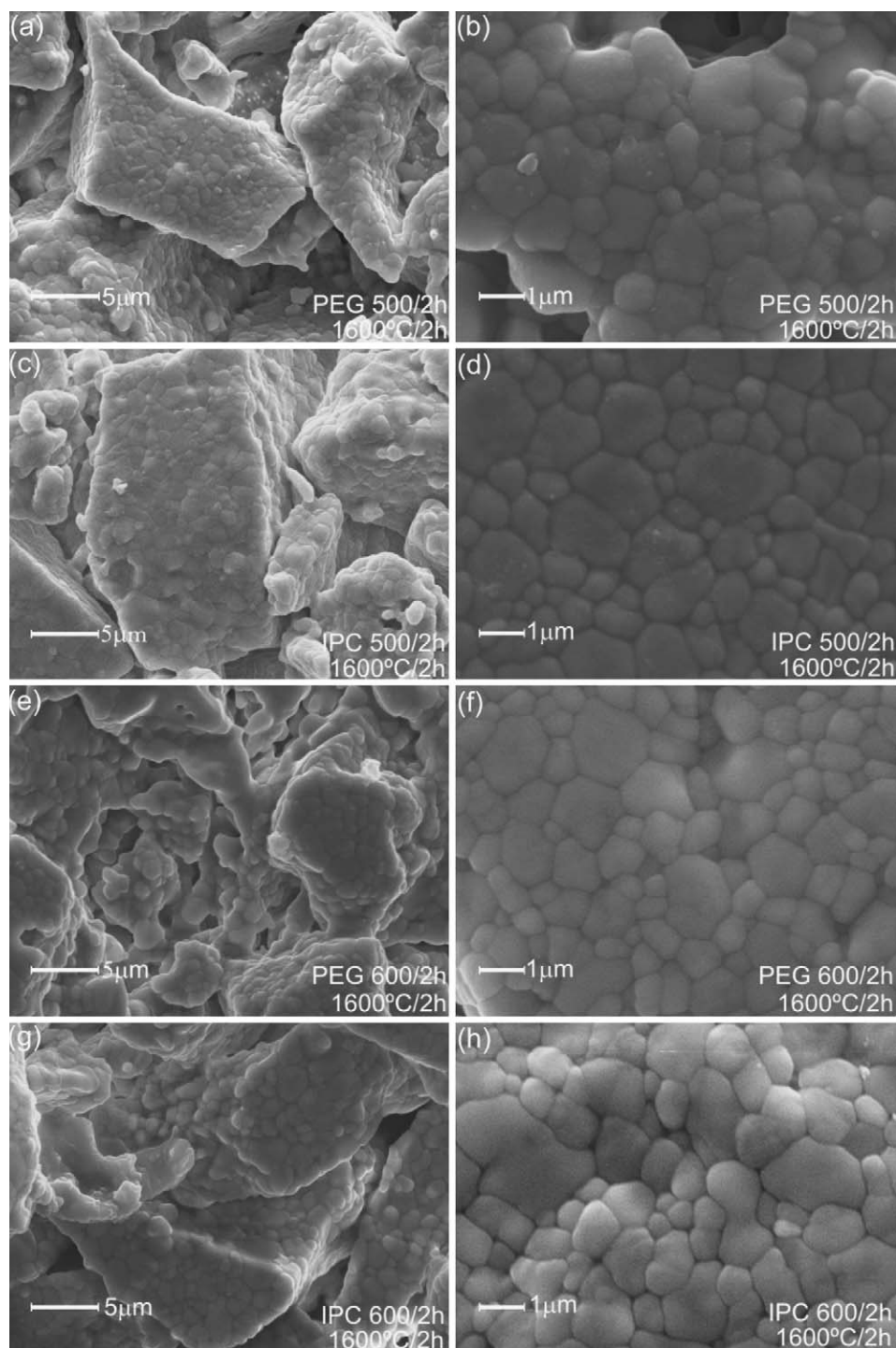


Fig. 6. Comparison of SEM micrographs of the IPC and PEG powders calcined at 1600 °C for 2 h: (a and b) PEG, (c and d) IPC; calcined at 500 °C for 2 h, (e and f) PEG, and (g and h) IPC; and calcined at 600 °C for 2 h.

The densified pellets were practically devoid of pores. However, the pores between the clusters were not eliminated, as indicated in Fig. 6, which shows that the microstructures obtained by the two methods and at every calcination time and temperature were very similar.

The grain size was not affected by either the method or the calcination conditions. Although the crystallites, which were

measured by the Scherrer method, presented nanometric sizes, the grains showed micrometric sizes.

All the sintered samples contained both coarse and small grains, possibly associated with cubic and tetragonal phases, respectively.

The XRD patterns of the sintered samples produced by the two methods showed tetragonal-cubic phase. Fig. 7 shows a

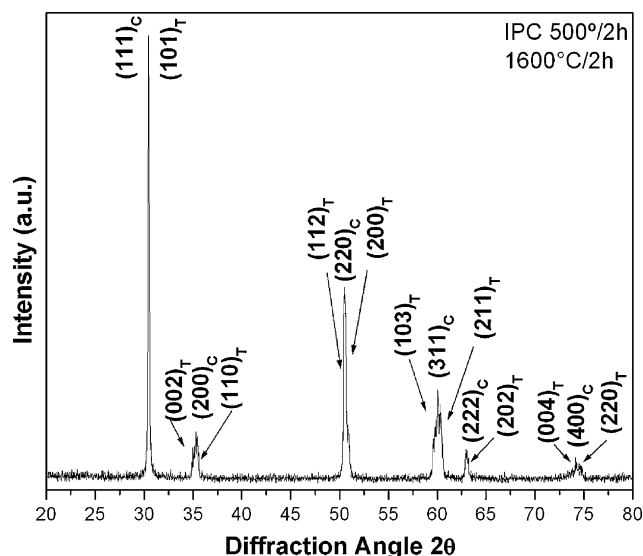


Fig. 7. Diffractogram of the IPC compacted powder calcined at 500 °C for 2 h, in the sintering schedule of 1550 °C/0 h–1300 °C/2 h.

diffractogram of the phases. All the sintered samples showed similar diffractograms, regardless of calcination temperature and time and the powder synthesis method.

4. Conclusion

FTIR spectroscopy revealed that coordination of metal ions with the polymer occurred in different ways, depending on the powder synthesis process.

The morphology of the powders differed only when organic impurities were not completely eliminated. After the complete elimination of organic impurities during calcination, the powders tended to form clusters of spherical-like particles, regardless of the synthesis method used. The powder synthesis method, calcination temperature and time changed the size of the resulting crystallites, and the most significant variation in crystallite size occurred when the calcination temperature was increased.

During sintering, the pellets densified and were practically devoid of pores, but the pores between clusters were not eliminated. The final grain size after sintering was in the order of 1 μm , remaining unaffected by the method of synthesis or the calcination conditions to which the powders were subjected. The presence of cubic and tetragonal phases of zirconia was observed by X-ray diffraction.

Acknowledgments

The authors gratefully acknowledge the Brazilian research funding agency CAPES for a scholarship and for its financial support of this work.

References

- [1] W.D. Kingery, J. Pappis, M.E. Doty, D.C. Hill, Oxygen ion mobility in cubic $\text{Zr}_{0.85}\text{Ca}_{0.15}\text{O}_{1.85}$, *J. Am. Ceram. Soc.* 42 (8) (1959) 393–398.
- [2] E.C. Subbarao, *Zirconia—An Overview*. Science and Technology of Zirconia, vol. 24, American Ceramic Society, Columbus, OH, 1981 pp. 1–22.
- [3] S.P.S. Badwal, F.T. Ciacchi, Oxygen-ion conducting electrolyte materials for solid oxide fuel cells, *Ionics* 6 (2000) 1–21.
- [4] D. Casellas, A. Feder, L. Llanes, M. Anglada, Fracture toughness and mechanical strength of Y-TZP/PSZ ceramics, *Scr. Mater.* 45 (2001) 213–220.
- [5] R. Stevens, *Zirconia and Zirconia Ceramics*, second edition, Magnesium Elektron Ltd., 1986.
- [6] J.W. Fergus, Electrolytes for solid oxide fuel cells, *J. Power Sources* 162 (1) (2006) 30–40.
- [7] Y. Chiang, D.P. Birnie III, W.D. Kingery, *Physical Ceramics: Principles for Ceramic Science and Engineering*, John Wiley and Sons, New York, 1997, 29–30.
- [8] J. Chavalier, L.T. Gremillard, The tetragonal-monoclinic transformation in zirconia: lessons learned and future trends, *J. Am. Ceram. Soc.* 92 (9) (2009) 1901–1920.
- [9] M. Bhagwat, V. Ramaswamy, Synthesis of nanocrystalline zirconia by amorphous citrate route: structural and thermal (HTXRD) studies, *Mater. Res. Bull.* 39 (2004) 1627–1640.
- [10] M.P. Pechini, US. Patent 3.330.697 (1967).
- [11] Y. Zhang, A. Li, Z. Yan, G. Xu, C. Liao, C. Yan, $(\text{ZrO}_2)_{0.85}(\text{REO}_{1.5})_{0.15}$ (RE = Sc, Y) solid solutions prepared via three Pechini-type gel routes. 1. Gel formation and calcinations behaviors, *J. Solid State Chem.* 171 (2003) 434–438.
- [12] Y. Zhang, A. Li, Z. Yan, G. Xu, C. Liao, C. Yan, $(\text{ZrO}_2)_{0.85}(\text{REO}_{1.5})_{0.15}$ (RE = Sc, Y) solid solutions prepared via three Pechini-type gel routes. 2. Sintering and electrical properties, *J. Solid State Chem.* 171 (2003) 439–443.
- [13] R.E.P. Salem, A.L. Chinelatto, A.S.A. Chinelatto, Sintering of Y_2O_3 -stabilized ZrO_2 powders obtained by different chemical methods, *Mater. Sci. Forum.* 591 (2008) 649–653.
- [14] B.D. Cullity, *Elements of X-ray Diffraction*, second edition, Addison-Wesley, Massachusetts, 1978.
- [15] J.D. Ballard, J. Davenport, C. Lewis, R.H. Domes, L.S. Schadler, W. Nelson, Phase stability of thermal barrier coatings made from 8 wt.% yttria stabilized zirconia: a technical note, *J. Thermal Spray Tech.* 12 (2003) 34–37.
- [16] S.G. Cho, P.F. Johnson, R.A. Condrate Sr, Thermal decomposition of (Sr,Ti) organic precursors during the Pechini process, *J. Mater. Sci.* 25 (1990) 4738–4744.
- [17] R.M. Silverstein, Identificação espectrométrica de compostos orgânicos comuns, Rio de Janeiro, Guanabara Koogan, 1994.
- [18] G.B. Deacon, R.J. Phillips, Relationships between the carbon-oxygen stretching frequencies of carboxylate complexes and the type of carboxylate coordination, *Coord. Chem. Rev.* 33 (1980) 227–250.
- [19] R.A. Rocha, E.N.S. Muccilo, Efeito da temperatura de calcinação e do teor de dopante nas propriedades físicas da céria-gadolínio preparada pela complexação de cátions com ácido cítrico, *Cerâmica* 47 (304) (2001) 219–224.